한국지진공학회 논문집 | 제12권 제1호 (통권 제59호) | 2008년 2월, pp. 43~55

# 복합감쇠모델을 이용한 비틂 시험기로 얻은 감쇠비에 상응하는 변형률 산정

# Identifying Strain Associated with Damping Ratio from Tosional Test Using a Combined Damping Model

배윤신[1)]

Bae, Yoon-Shin

**국문 요약 >>** 비틂시험에서 전단탄성계수와 감쇠비에 상응하는 변형률 산정의 복잡성은 여러 방법에 의하여 해결되어 왔다. 특히, 수정 등가반경법은 공진주/비틂전단 시험의 모든 변형률 영역에서 변형률에 따른 등가반경비 곡선을 보다 효과적으로 나타내는데 적합하다. 감쇠비 산정시 수정 등가반경법을 쌍곡선 모델, 수정 쌍곡선 모델, 램버그오스굿 모델등에 적용시켜 보았다. 연구결과는 감쇠비 산정시 재래식 등가반경법에 의한 하나의 등가반경 수치를 사용하는 것은 적절치 않다는 것을 보여주었다. 이력감쇠뿐 아니라 미소변형률 영역에서의 흙의 감쇠 현상을 고려하기 위하여 새로운 모델이 개발되었고, 이러한 두 가지 복합감쇠에 상응하는 변형률 산정시 부가적 조정이 필요한지 검토해 보았다.

**주요어** 감쇠비, 비선형 지반 모델, 변형율 계산

**ABSTRACT >>** The complexity of determining strain associated with shear modulus and damping ratio in torsional tests has been resolved by means of several approaches. Particularly, the modified equivalent radius approach is adequate to when generating the plots of equivalent radius ratio versus strain more effectively over any range of strains in resonant column and torsional shear (RC/TS) tests. The modified equivalent radius approach was applied for hyperbolic, modified hyperbolic, and Ramberg-Osgood models in evaluating damping ratio. Results showed that using a single value of equivalent radius ratio based on conventional equivalent radius approach is not appropriate. A new model was developed to consider the soil damping behavior at small strains as well as hysteretic damping and it was attempted to determine adjustments are required in evaluating strain associated damping when combining the two damping components.

**Key words** damping ratio, nonlinear soil model, strain calculation

## 1. INTRODUCTION

When a soil specimen is subjected to cyclic loading in torsional tests, hysteresis loops generated in the torque-twist plane provide energy dissipation due to hysteretic behaviour. Effective damping ratio is defined as the energy dissipated in the area loops divided by the areas of the triangle in the torque-twist plane. Evaluation of damping requires identification of a specific strain associated with the effective damping ratio at given twist. Hence, attempts have been made to deal with nonuniform stress-strain effects occurring over the radius of soil specimen in the resonant column and torsional sherar (RC/TS) test with an equivalent radius approach by Chen and Stokoe[(1)] and modified equivalent radius approach by Sasanakul[(2)].

In this study, the modified equivalent radius approach was extended to damping ratio using both the modified hyperbolic model (Darendeli and Stokoe[(3)]) and Ramberg -Osgood model (Ishihara[(4)]). Damping ratio is calculated from hysteresis loop assuming Masing rules[(5)].

[1)] 정회원·유타주립대학교 박사과정
(대표저자: yoshbae@hanmail.net)

본 논문에 대한 토의를 2008년 4월 30일까지 학회로 보내 주시면 그 결과를 게재하겠습니다.

(논문접수일 : 2007. 11. 16 / 심사종료일 : 2008. 1. 15)

Soil damping behavior is described in several aspects. It is known that soils generally exhibit constant damping for strains in the linear range, but increasing damping as strains increase into the nonlinear range. And damping in soil is generally constant with frequency of loading[6]. Several models are used to describe these damping behaviors of soil but no single mechanistic damping model has all of these behaviors. A viscous model is used to describe the energy loss due to nonhysteretic behavior, which is called viscous damping. Two weaknesses of the model is that it lacks in describing the hysteretic damping behavior and rate-independent nature of soil damping. On the other hand, hysteretic model describes the energy loss due to nonlinear stress-strain relationship. However, it does not contain the damping ratios at small strains.

Each of these models describes part of soils actual damping behavior but none of them completely describe the combined damping behavior. Hence, a combined hysteretic-nonviscous model was developed and employed to determine if any adjustments are needed in applying the modified equivalent radius approach to measured damping considering of both hysteretic and nonviscous components.

## 2. EQUIVALENT RADIUS APPROACH BY CHEN AND STOKOE (1979)

### 2.1 Investigation of Damping from Torsional Soil Tests

Dealing with linearly varying strains in torsional testing is complicated and one of the weaknesses in the RC/TS testing. Chen and Stokoe[1] developed an equivalent radius approach to account for the the nonuniform distribution of strain in the soil specimen.

When a soil element is subjected to cyclic loading, it generates hysteresis loop on the stress-strain plane as shown in Figure 1 and hysteretic damping ratio, D, is defined as:

$$D = \frac{A_L}{4\pi \cdot A_T}, \quad (1)$$

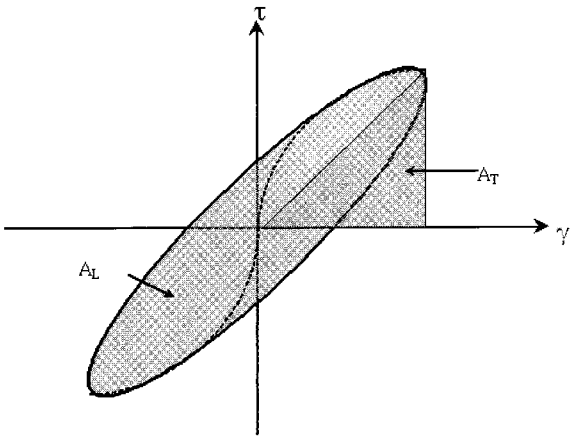


〈Figure 1〉 Definition of hysteretic damping

where, $A_L$ = the areas of the loop, and
$A_T$ = the areas of the triangle.

When a soil specimen is subjected to torsional loading, hysteresis loops are measured in the torque-twist plane. The effective hysteretic damping ratio, $D_{eff}$, can be calculated similarly following Equation 1 except that the damping calculated in this way is associated with a given twist, $\theta$, and not with a strain, $\gamma$.

To obtain the hysteresis loop, it is assumed that the soil behaves according to Masing behavior. Once the hysteresis loops have been determined, damping ratio, D and effective damping ratio, $D_{eff}$ are determined from the area of the loop as shown in Equation 1 and Figure 1.

There are two notable differences between the hysteretic damping ratio and actual soil damping ratio. First, damping calculated based on Masing behavior lacks small-strain damping, $D_{min}$. Second, the asymptote of hysteretic damping has a value of $2/\pi$ or 63.7 percent. This value is much larger than those predicted by Seed and Idriss[7] or Hardin and Drnevich[8]. However, Chen and Stokoe[1] indicated that the strains at which hysteretic damping approaches this asymptote are also much larger than the strains which were used in typical tests. They also stated that if high strain tests (1 to 5 percent) are performed, then the calculated hysteretic damping value is 30 to 55 percent which is in good agreement with theoretical maximum values.

They compared the effective hysteretic damping ratio, $D_{eff}$ determined from solid sample with hysteretic

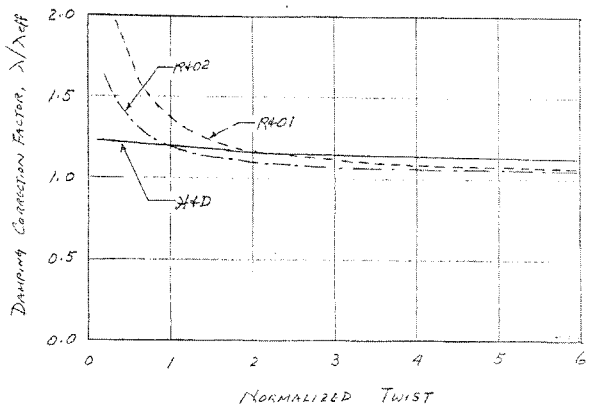


〈Figure 2〉 Damping correction factors for solid specimen (from Chen and Stokoe, 1979)

Note: $\lambda$ = hysteretic damping ratio, D and $\lambda_{eff}$ = effective hysteretic damping ratio, $D_{eff}$

damping ratio, D, from the stress-strain curves. Figure 2 presents the ratio of D to $D_{eff}$ with respect to normalized twist, $\theta/\theta_r$. The reference rotation, $\theta_r$ is defined as reference strain, $\gamma_r$ multiplied by specimen height, L divided by specimen radius, r. It shows that effective damping ratio, $D_{eff}$ is always smaller than damping ratio, D at the strain at the periphery of the sample for a given twist, $\theta$.

An equivalent radius ratio, $R_{eq}$, which is defined as the ratio of the equivalent radius and the radius of soil specimen was used to relate $D_{eff}$ with D as well as $G_{eff}$ with G. The same equivalent radius ratio, $R_{eq}$, was used for damping ratio as was used for shear modulus. A value for the equivalent radius ratio of about 0.82 times the outside radius is a good estimate for torsional testing below 0.001 (%) strain and 0.79 for between 0.001 (%) and 0.1 (%) strains.

### 2.2 Weaknesses of the Equivalent Radius Ratio

There are two weaknesses in using equivalent radius ratio, $R_{eq}$, to determine damping ratio. The first weakness is that it does not account for differences in nonlinearity in different soils. The nonlinearity in soil can be expressed relative to reference strain, $\gamma_r$ using equation (Pyke[9]):

$$\gamma_r = \frac{\tau_{max}}{G_{max}}, \qquad (2)$$

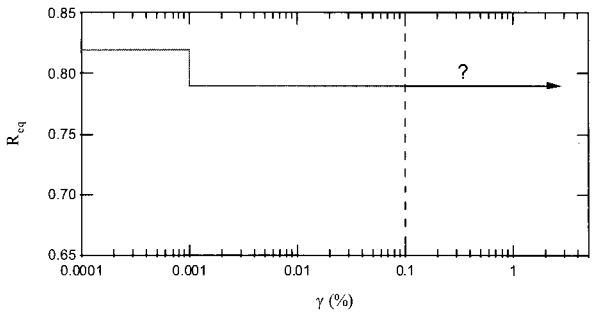


〈Figure 3〉 $R_{eq}$ values based on damping from Chen and Stokoe (1979)

where, $\tau_{max}$ = maximum shear stress, and

$G_{max}$ = shear modulus at low strains.

Soils with larger values of reference strain have greater shear strengths relative to their small strain moduli and show more elastic, less nonlinear, stress-strain behavior than soils with smaller values of reference strain. Figure 3 shows the Chen and Stokoe[1] recommended values for $R_{eq}$, which are independent of reference strain. The second weakness is that the Chen and Stokoe[1] approach developed the value of $R_{eq}$ based upon shear modulus but it is also used to calculate strain in damping measurements. Sasanakul and Bay[10] demonstrated that is not accurate.

## 3. MODIFIED EQUIVALENT RADIUS APPROACH

A more general approach to account for nonuniform stress-strain than the conventional equivalent radius approach, the modified stress integration approach was developed[2]. The nonuniform stress-strain was accounted for more precisely by integrating the stress over the radius of soil specimen to obtain a twist-torque relationship. A theoretical twist-torque relationship was developed using closed form integration with hyperbolic model[2], or numerical integration using the modified hyperbolic model or Ramberg-Osgood model[11].

It is believed that hysteresis loops do not alone provide the mechanism of all damping for soils. Hence, a certain amount of viscous (or nonviscous) damping should be considered in addition to hysteretic damping in nonlinear analyses[12]. A combined damping model describing nonviscous and hysteretic damping was

developed to better approximate soil behavior[11]. The new combined damping model was employed to determine adjustments are required when combining the two soil damping behaviors.

### 3.1 $R_{eq}$ Based on Hyperbolic Model

To determine values of $R_{eq}$, it is required to generate D versus $\gamma$ curve and $D_{eff}$ versus $\theta$ curve. The twist-torque relationship was calculated using closed form integration developed by Sasanakul[2]. The closed form solution was obtained assuming the stress-strain relation is hyperbolic. The stress-strain relationship and the closed form solution of torque-rotation relationship are presented in Equation 3 and 4, respectively.

$$\tau = \frac{G_{max}\gamma}{1+\left(\frac{\gamma}{\gamma_r}\right)} \tag{3}$$

where, $G_{max}$ = shear modulus at low strain.

$$T = \frac{1}{3}\pi G_{max}\gamma_r r\left[2r^2 - 3r\left(\frac{\gamma_r L}{\theta}\right) + 6\left(\frac{\gamma_r L}{\theta}\right)^2\right] + 2\pi G_{max}\gamma_r^4\left(\frac{L}{\theta}\right)^3\left[\ln(\gamma_r) - \ln\left(\gamma_r + \frac{\theta r}{L}\right)\right] \tag{4}$$

where, T = torque,
r = radius of soil specimen,
L = height of soil specimen, and
$\theta$ = rotation.

Assuming the soil behaves according to Masing behavior, the hysteretic damping ratio is calculated by the equation[4]:

$$D = \frac{2}{\pi}\left[\frac{2\int_0^{\gamma}\tau(\gamma)d\gamma}{\gamma\tau(\gamma)} - 1\right] \tag{5}$$

By introducing Equation 3 into Equation 5, the damping

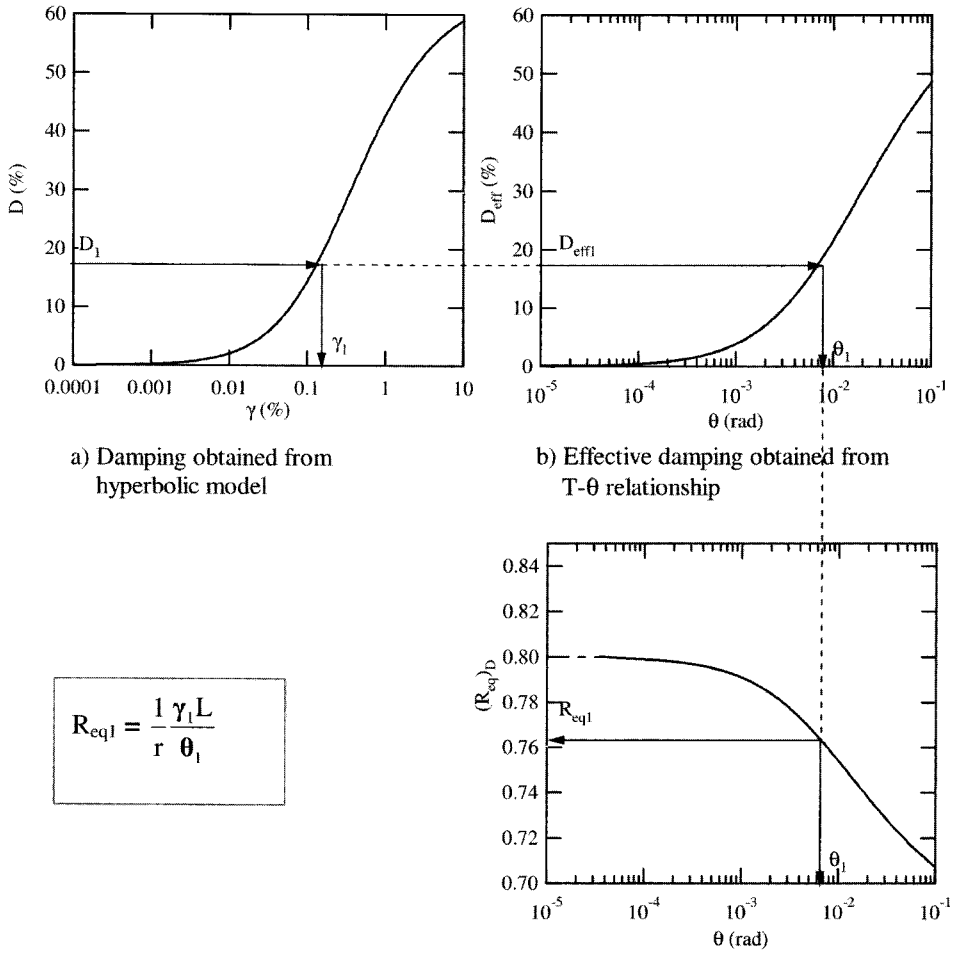


a) Damping obtained from hyperbolic model

b) Effective damping obtained from T-θ relationship

c) $(R_{eq})_D$ ratio curve based on damping

$$R_{eq1} = \frac{1}{r}\frac{\gamma_1 L}{\theta_1}$$

〈Figure 4〉 Determination of $R_{eq}$ based on damping ratio (from Sasanakul 2005)

ratio, D can also be expressed as:

$$D = \frac{4}{\pi}\left[1+\frac{1}{\gamma/\gamma_r}\right]\left[1-\frac{\ln(1+\gamma/\gamma_r)}{\gamma/\gamma_r}\right]-\frac{2}{\pi} \quad (6)$$

Equation 6 was used to generate the D-$\gamma$ curve using hyperbolic model shown in Figure 4a.

The twist-torque relationship is obtained using Equation 4. The low strain shear modulus, $G_{max}$ used in this analysis is 47,880 kPa. Using the twist torque relationship, the effective damping raio, $D_{eff}$ is obtained with the following equation:

$$D_{eff} = \frac{2}{\pi}\left[\frac{2\int_0^{\theta} T(\theta)d\theta}{\theta T(\theta)}-1\right] = \frac{1}{4\pi}\left[\frac{8(\int_0^{\theta} T(\theta)d\theta - \frac{1}{2}\theta T(\theta))}{\frac{1}{2}\theta T(\theta)}\right] \quad (7)$$

Equation 7 was used to generate the $D_{eff}$-$\theta$ curve shown in Figure 4b.

The steps to determine values of $R_{eq}$ are as follows. The damping ratio, $D_1$ corresponding to a given shear strain, $\gamma_1$ can be obtained from Figure 4a. A value $\theta_1$ that is associated with the $D_{eff}$ value equal to $D_1$ is determined in Figure 4b. Then using Equation 8, a value of $R_{eq}$ is calculated as shown in Figure 4c, using:

$$R_{eq} = \frac{1}{r}\frac{\gamma L}{\theta} \quad (8)$$

The $R_{eq}$ curves based on damping ratio is shown in Figure 5 with $R_{eq}$ curves based on shear modulus [2]. The procedure to determine $R_{eq}$ curves based on shear modulus is described in detail by Sasanakul [2].

As shown in Figure 5, several advantages using modified equivalent radius approach to determine $R_{eq}$ values are as follows:

1. The conventional equivalent radius approach uses single values of $R_{eq}$ irrespective of reference strain, $\gamma_r$ and shear strain, $\gamma$. The actual $R_{eq}$ decreases with increasing strains and the point where the $R_{eq}$ decreases is associated with the value of reference rotation, $\theta_r$, which is defined as Equation 9. Therefore, the equivalent radius approach accounts for this variation of $R_{eq}$ over the range of strains and the soil nonlinearity.

$$\theta_r = \frac{\gamma_r L}{r} \quad (9)$$

2. The conventional equivalent radius approach was limited at strain levels up to 0.1% while the modified equivalent radius approach can be applied for high strains.
3. The conventional equivalent radius approach developed the value of $R_{eq}$ on shear modulus and the values are also applied for the determination of strains for damping. As shown in Figure 5, the $R_{eq}$ values for damping is less than the $R_{eq}$ values for shear modulus and the difference increases as the strain level increases. Hence, the modified equivalent approach provides more precise damping curves in RC/TS testing.

### 3.2 $R_{eq}$ Based on Modified Hyperbolic Model

The modified equivalent radius approach was extended to generate $R_{eq}$ values for damping using modified hyperbolic model. To obtain $R_{eq}$ based on modified hyperbolic stress-strain relationship, the approach starts by numerically relating the shear stress, $\tau$ acting on a circular cross section to strain, $\gamma$ using:

$$\tau = \frac{G_{max}\gamma}{1+\left(\frac{\gamma}{\gamma_r}\right)^a}, \quad (10)$$

where, $G_{max}$ = shear modulus at low strain (47,880 kPa),
a = curvature coefficient, and
$\gamma_r$ = reference strain.

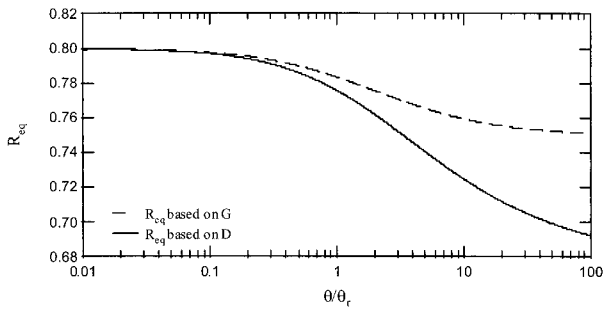


〈Figure 5〉 $R_{eq}$ curves based on G and D (from Sasanakul 2005)

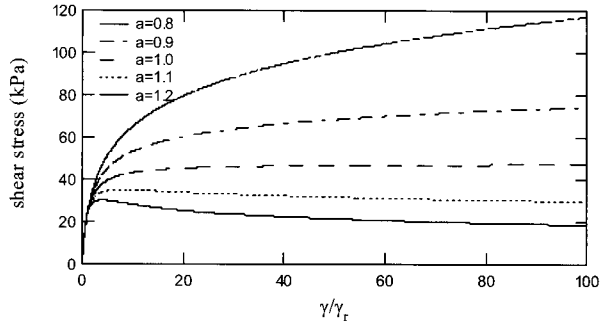


〈Figure 6〉 Stress strain curves for modified hyperbolic model with different curvature coefficients

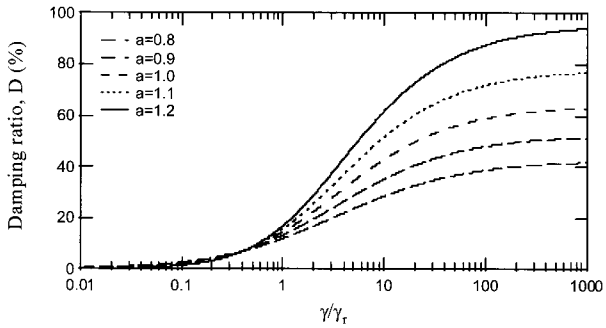


〈Figure 7〉 Damping ratio for modified hyperbolic model

The stress strain curves for different curvature coefficients are presented in Figure 6, using strain normalized with respect to reference strain.

To generate the D-γ curve numerically, Equation 5 was employed using Equation 10. The Figure 7 shows the D-γ curve for modified hyperbolic model, again using normalized strain.

The T-θ relationships were then determined numerically using Equation 11:

$$T = \int_A dM = \int \tau r dA = \int_0^r 2\pi r^2 \tau dr \quad , \tag{11}$$

where, M = resultant moment over the entire cross section area,

A = cross section area, and

τ = shear stress obtained using Equation 10.

Sasanakul[2] presented the numerical procedure obtaining torque for given stress-strain relationship based on modified hyperbolic model. For a given twist, θ, the relationship between radius, r and shear strain, γ can be

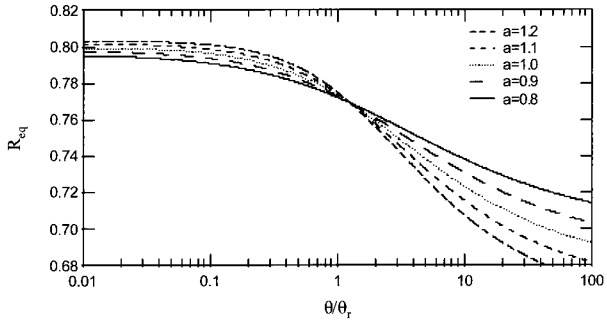


〈Figure 8〉 $R_{eq}$ curves based on damping with modified hyperbolic model

obtained using Equation 12.

$$r = \frac{L}{\theta}\gamma \tag{12}$$

Then, the relationship between the differential of strain, dγ, and the differential of radius, dr, is as follows:

$$dr = \frac{L}{\theta}d\gamma \tag{13}$$

Substitution of Equation 12 and 13 into Equation 11 and changing the upper limit of integration to $\gamma_{max}$ corresponding to exterior radius gives, r:

$$T = 2\pi\left(\frac{L}{\theta}\right)^3 \int_0^{\gamma_{max}} \tau(\gamma)\gamma^2 d\gamma \quad , \tag{14}$$

where, $\tau(\gamma)$ is stress-strain relationship based on Equation 10.

And, the effective damping ratio was obtained by numerical integration using Equation 7.

After obtaining the effective damping ratio, $D_{eff}$, the same procedures presented in Figure 4 are applied to determine $R_{eq}$ based on modified hyperbolic model.

Figure 8 presents the $R_{eq}$ based on damping ratio with modified hyperbolic model using different curvature coefficients. Rotations are normalized with respect to reference rotation, $\theta_r$, as defined in Equation 9. As shown in Figure 8, the ranges of $R_{eq}$ value are wider at high strains.

### 3.3 $R_{eq}$ Based on Ramberg-Osgood Model

The modified equivalent radius approach was also

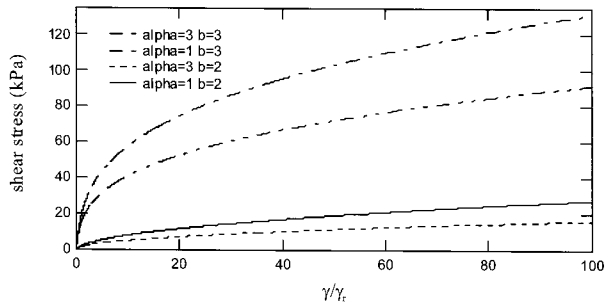


〈Figure 9〉 Stress strain curves for Ramberg-Osgood model with different model parameters (α, b)

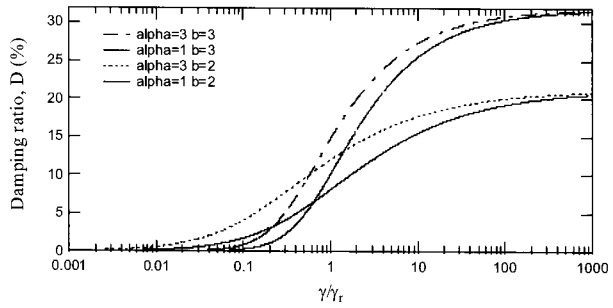


〈Figure 10〉 Damping ratio for Ramberg-Osgood model

extended to generate $R_{eq}$ values for damping using Ramberg-Osgood model. To obtain $R_{eq}$ based on Ramberg-Osgood stress-strain relationship, the approach starts by numerically relating the shear stress, $\tau$ acting on a circular cross section to strain, $\gamma$ using:

$$\gamma = \frac{\tau}{G_{max}}\left(1+\alpha\left|\frac{\tau}{G_{max}\gamma_r}\right|^{b-1}\right) \quad (15)$$

The model parameters for Ramberg-Osgood model are: $G_{max}$, $\gamma_r$, $\alpha$, and b. The reference strain is the same as the reference strain used in the hyperbolic model. The stress strain curves, relative to normalized strain, for different model parameters ($\alpha$ and b) are presented in Figure 9. The damping ratio from this Ramberg-Osgood formulation can be explicitly expressed as a function of parameters, ($\alpha$ and b) as:

$$D = \left[2\alpha(b-1)(\tau/G_{max}\gamma_r)^b\right]/\left[\pi(b+1)(\gamma/\gamma_r)\right] \quad (16)$$

Figure 10 shows the D-$\gamma$ curve based on Equation 16.

Torque for Ramberg-Osgood model was also obtained numerically[2]. The Ramberg-Osgood model presents $\gamma$ as a function of shear stress, $\tau$. For a given twist, $\theta$, the relationship between radius, r and shear strain, $\gamma$ can be obtained using Equation 12. Then, radius, r can be expressed as:

$$r = \frac{L}{\theta}\frac{\tau}{G_{max}}\left[1+\alpha\left|\frac{\tau}{G_{max}\gamma_r}\right|^{b-1}\right] \quad (17)$$

Torque is calculated numerically integrating the stress-strain relationship using:

$$T = 2\pi\int_0^r \tau(\mathbf{r})\mathbf{r}^2 dr \quad , \quad (18)$$

where, $\tau(\gamma)$is stress-strain relationship based on Equation 15. And the effective damping ratio was obtained by numerical integration using Equation 7.

After obtaining the effective damping ratio, $D_{eff}$, the same procedures presented in Figure 4 are applied to determine $R_{eq}$ based on Ramberg-Osgood model.

Figure 11 presents the $R_{eq}$ relative to normalized rotation based on damping ratio with Ramberg-Osgood model using model parameters ($\alpha$ and b). Figure 11 shows that the scatter of $R_{eq}$ values in high strain range is less than the scatter in $R_{eq}$ values for the modified hyperbolic model. But the range of $R_{eq}$ value is increased in lower strain range.

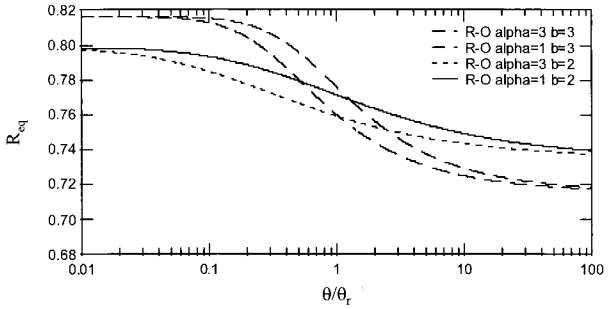


〈Figure 11〉 $R_{eq}$ curves based on D with Ramberg-Osgood model

### 3.4 $R_{eq}$ Based on Combined Model

So far the correction of material damping is based on the assumption that the measured damping is hysteretic only. Hysteresis loop, however, do not alone provide the

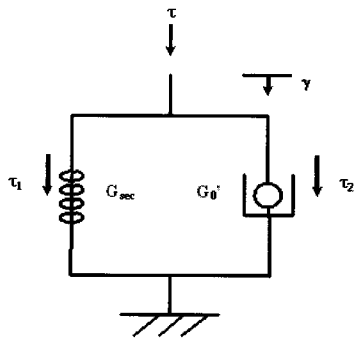


〈Figure 12〉 Nonviscous type model with nonlinear spring showing τ vs. γ

mechanism of all damping for soils particularly at small strains, and a certain amount of viscous (or nonviscous) damping should be considered in addition to hysteretic damping in a nonlinear analyses. Hence, a new model was developed and employed to determine adjustments are required when combining the two damping components.

To consider two components, a nonlinear spring with a varying spring constant, $G_{sec}$ and rate independent dashpot, $G_0'$ were employed shown in Figure 12. The nonlinear spring constant, $G_{sec}$ is the secant modulus calculated by using hyperbolic model. To eliminate frequency dependence, rate independent dashpot, $G_0'$ was introduced. The rate independent dashpot, $G_0'$ can be calculated using $G_{sec}$ determined for specific shear strain using:

$$G_0' = 2 \cdot G_{sec} \cdot D_{min} \tag{19}$$

where, $G_{sec}$ = secant modulus based on hyperbolic model and

$D_{min}$ = nonviscous damping occurred at low strains.

Then the total stress, $\tau = (G_{sec} + iG_0')\gamma$, was obtained at several strain levels. The imaginary term is used because $\tau_2$ is 90 ° out of phase with $\tau_1$.

To plot the stress induced by the dashpot ($\tau_2$), it is required to plot each stress component in time domain. Hence stress caused by non-linear spring ($\tau_1$), stress induced by the dashpot ($\tau_2$), and total stress ($\tau = \tau_1 + \tau_2$) was plotted in terms of period, $(\omega t/2\pi)$ in Figure 13. Figure 13 shows the results based on a maximum shear strain of 0.63 % and $D_{min}$ of 2 %. Figure 14 presents the total stress ($\tau = \tau_1 + \tau_2$) vs strain.

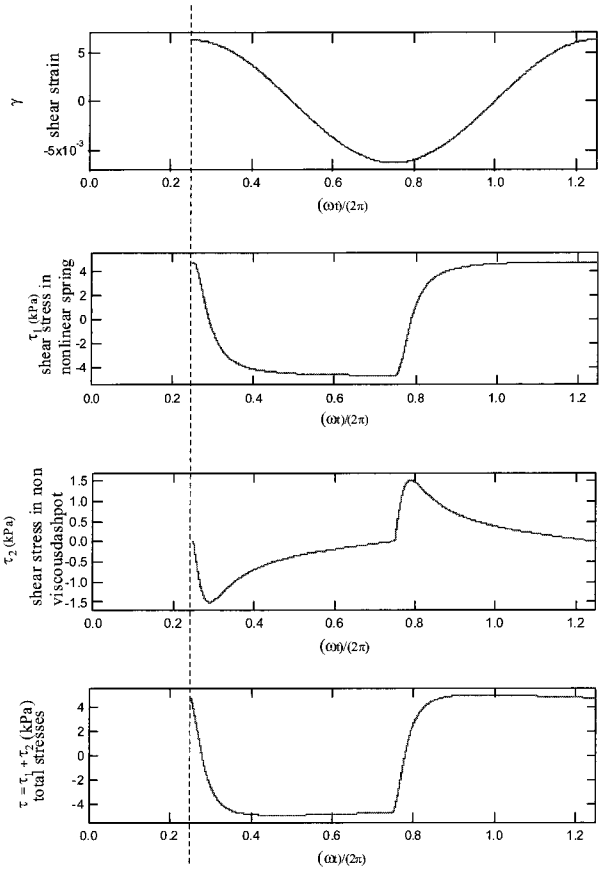


〈Figure 13〉 Strain, and stresses determined by nonlinear shear modulus and dashpot for a maximum rotation of 0.63 %

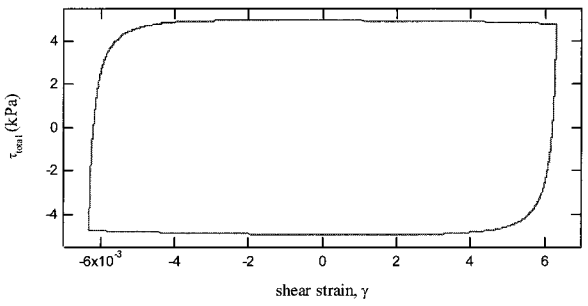


〈Figure 14〉 Total stress vs strain

The damping ratio using combined nonviscous hyperbolic nonlinear model then can be calculated by using following equation:

$$D = \frac{A_L^*}{4\pi A_T}, \tag{20}$$

where, $A_L^*$ = area inside the loop generated by total stress and shear strain, and

$A_T$ = area of the triangle.

Figure 15 presents the calculation of damping ratio for the combined hysteretic and nonviscous damping. The dotted line indicated the hysteresis loop based on the hyperbolic nonlinear stress-strain relationship without considering damping at low strains, $D_{min}$.

The effective damping ratio can also be computed using Equation 20. However, effective damping computed in this manner is associated with rotation, $\theta$, and $T_{total}$. To define total torque ($T_{total}$), a mechanical analog is introduced in Figure 16. Total torque, $T_{total}$ is defined as summation of torque in the nonlinear spring ($G_{eff}$), $T_1$ and the torque in the nonviscous dashpot ($G_0^*$), $T_2$.

At a given rotation, $T_1$ can be obtained from the closed form integration of the twist-torque relationship in Equation 4. By linearizing the problem, $T_2$ can be determined using the equation:

$$T_2 = \frac{G_0^* I_p}{L} i\theta, \tag{21}$$

where, $G_0^* = 2 \cdot Dmin \cdot G_{eff}$.

The imaginary term is also used because $T_2$ is 90 ° out of phase with $T_1$.

To plot the $T_2$ induced by the dashpot, it is also required to plot each torque component in time domain. Therefore, rotation, $T_1$, $T_2$, and total torque T, ($T = T_1 + T_2$) are plotted in terms of period, $\omega t/2\pi$ in Figure 17. Figure 17 presents the results based on a rotation of 0.0252 rad and $D_{min}$ of 2 %. Figure 18 shows the total torque ($T = T_1 + T_2$) vs rotation, $\theta$.

A procedure to determine $R_{eq}$ based on combined non-viscous hyperbolic non-linear model is illustrated in Figure 19. Using Equation 20, damping ratios, D are obtained at several strains shown in Figure 19a. Figure 19b shows the curve fitting technique applied to obtain

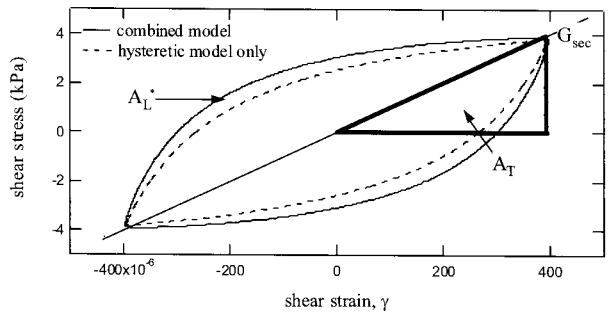


〈Figure 15〉 Calculation of damping ratio combined hysteretic and nonviscous damping

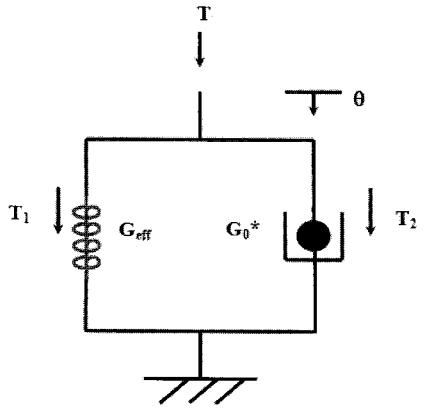


〈Figure 16〉 Nonviscous type Kelvin model with nonlinear spring showing T vs. θ

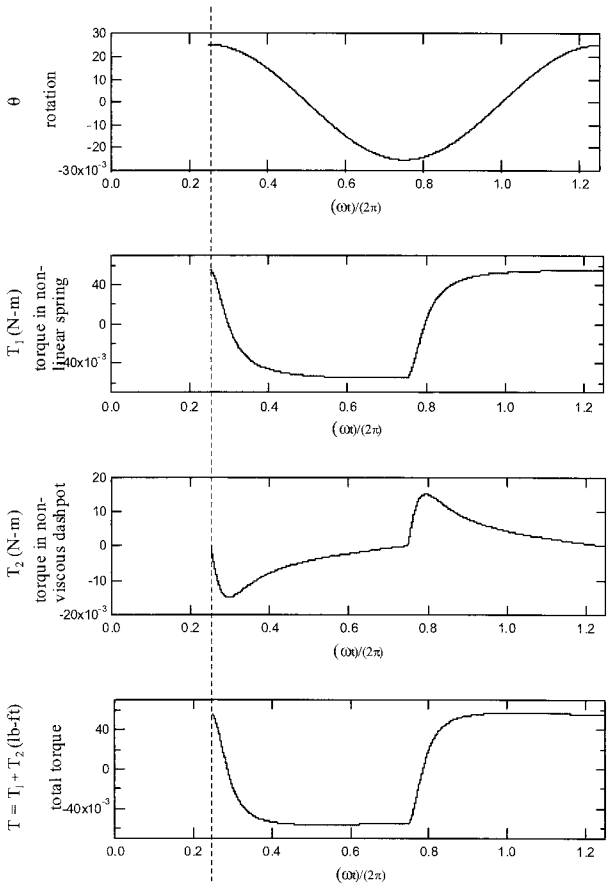


〈Figure 17〉 Rotation, and torques determined by effective shear modulus and dashpot for a maximum rotation of 0.0252 radians

D-γ curve. For a given rotation, $\theta_1$, effective damping ratio, $D_{eff}$ is obtained shown in Figure 19c. The shear strain, $\gamma_1$ at which D equals $D_{eff}$ in the τ–γ relation is obtained as shown in Figure 19d. $R_{eq1}$ at given $\theta_1$ is calculated using Equation 8 shown in Figure 19e.

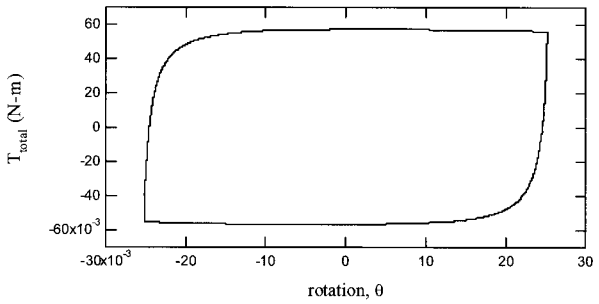


〈Figure 18〉 Total toque vs rotation

The same procedures are repeated at several rotations and $R_{eq}$ values at several rotations in case of $D_{min}$ equal to 4 % are shown in Figure 20. Figure 21 presents $R_{eq}$ values based on damping with viscous damping, $D_{min}$=0.5, 1.0, 2.0, 4.0 %, respectively. The dotted line in Figure 21 is the $R_{eq}$ values for damping from Figure 5, obtained from only hysteretic damping. It can be seen in Figure 21, that damping ratio at small strain, $D_{min}$ does not effect the $R_{eq}$ values.

## 4. APPLYING THE MODIFIED EQUIVALENT RADIUS APPROACH TO RC/TS TESTING

The RC/TS tests measure torque-rotation relationship. The theoretical torque-rotation relationship can be

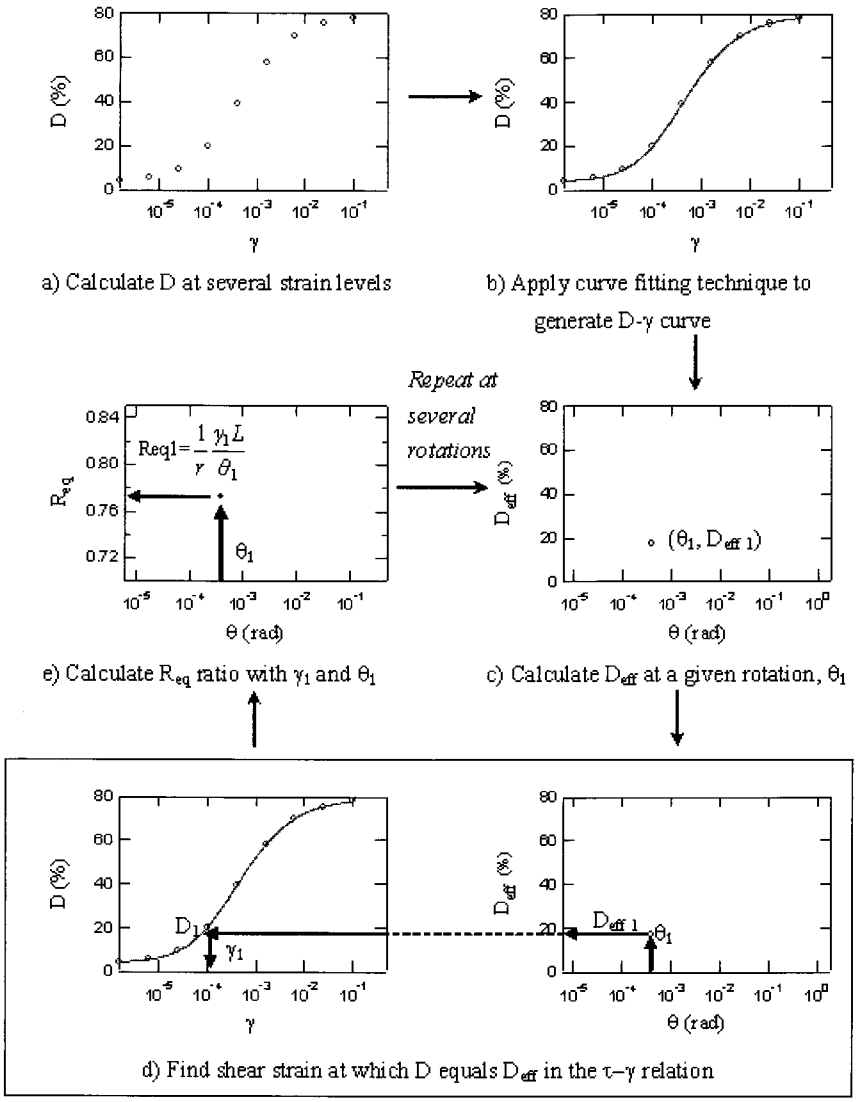


〈Figure 19〉 Determination of $R_{eq}$ based on combined nonviscous hyperbolic nonlinear model

obtained by closed form solution or numerical method shown in Equations 4, 14, and 18, respectively. Curve fitting techniques[2] are then used to match the theoretical torque-rotation relationship with the measured torque-relationship to obtain the best fit model parameters. The model parameters are used to develop the stress-strain relationship for soil. The $R_{eq}$ curves based on damping ratio are then determined using the stress-strain relationship.

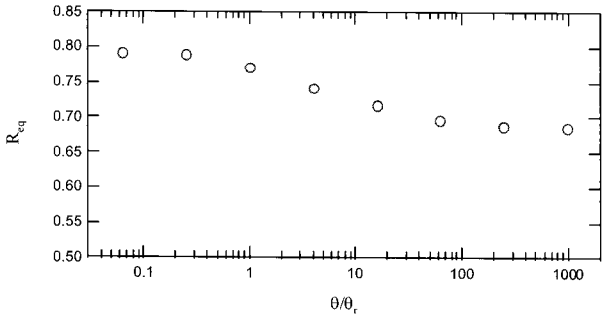


〈Figure 20〉 $R_{eq}$ values based on damping with viscous damping, $D_{min}$ = 4 %

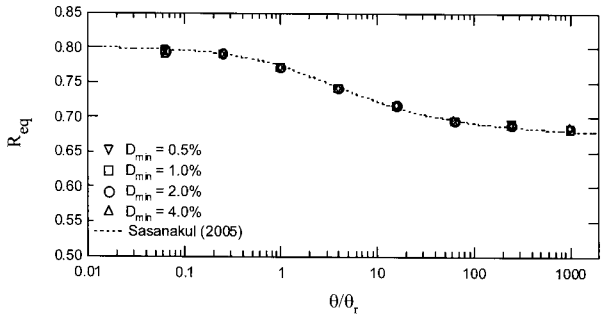


〈Figure 21〉 $R_{eq}$ values based on damping with viscous damping, $D_{min}$ = 0.5, 1.0, 2.0, 4.0 %, respectively

Effective damping of soil is determined using the half power band width method or the free vibration decay method for the RC tests. The area of the hysteresis loop is used to determine effective damping in TS tests. It has been shown that for soils with elliptical hysteretic stress-strain curves, material damping measured using these two tests should be identical[13].

A summary of the application of modified equivalent radius approach for damping calculations in TS testing is presented in Figure 22.

The methods for calculating damping ratio using half power band width method are described in detail[14]. The damping ratio can be calculated using Equation 22.

$$D \approx \frac{f_2 - f_1}{2f_n} . \qquad (22)$$

where $f_n$ = resonant frequency, and

$f_1$ and $f_2$ = two points on the response curve at M is equal to $1/\sqrt{2}\, M_{max}$.

Figure 23 summarized application of the modified equivalent radius approach to the half power band width method.

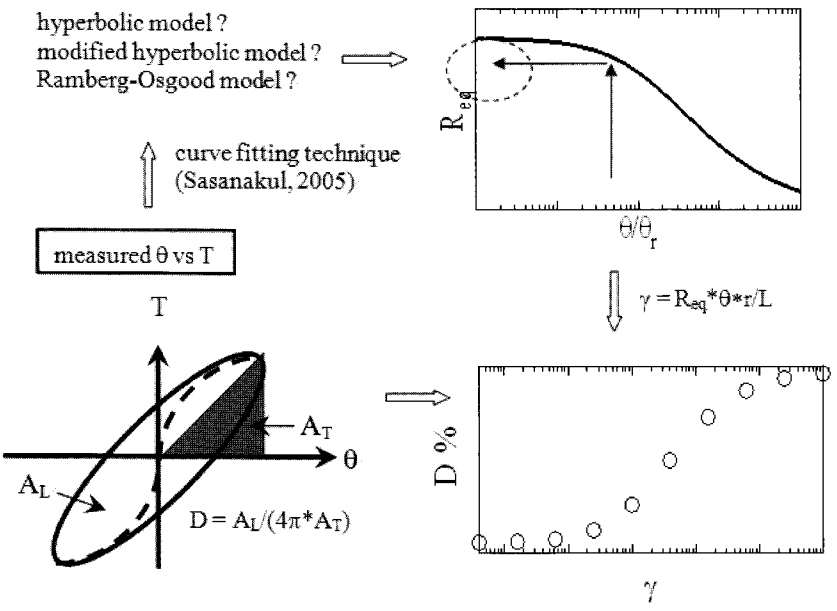


〈Figure 22〉 Summary of the application of the modified equivalent radius approach to torsion shear tests

Free vibration decay is the method used to determine damping utilizing the decay of vibration at resonance[14]. The natural logarithm of two successive amplitude of motion is called the logarithmic decrement, $\delta$ expressed as:

$$\delta = \frac{2\pi D}{\sqrt{1-D^2}}. \quad (23)$$

Equation 23 can be used for calculating the material damping, D using the free vibration decay method.

The modified equivalent radius approach is applied by using the following equation to determine the strain, $\gamma$, corresponding to a measured effective damping ratio in rotation-time domain during free vibration decay:

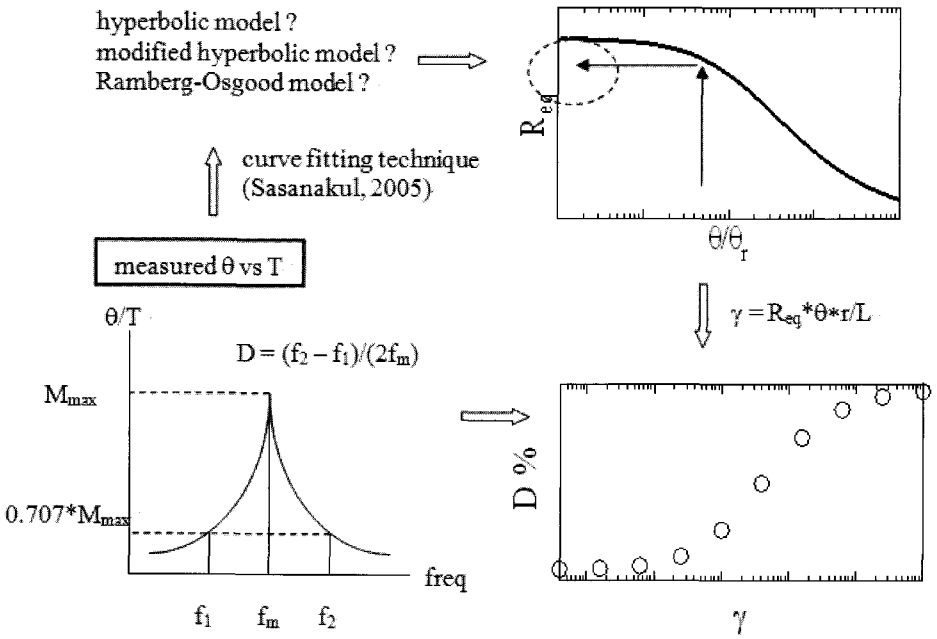


〈Figure 23〉 Summary of the application of the modified equivalent radius approach to half power band width method in RC testing

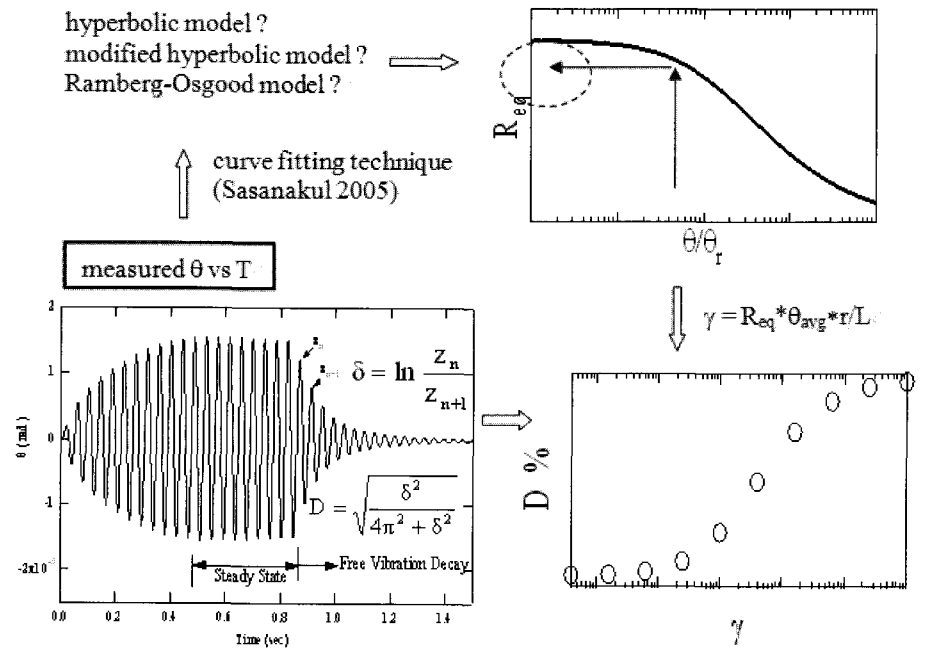


〈Figure 24〉 Summary of the application of the modified equivalent radius approach to free vibration decay method in RC testing

$$\gamma = R_{eq}\frac{\theta_{avg} r}{L}, \quad (24)$$

where, $\theta_{avg}$ = average of the first three cycles of the free vibration decay curve.

Figure 24 shows the summary of application of the modified equivalent radius approach to the free vibration decay method.

## 5.CONCLUSIONS

The modified equivalent radius approach was applied using the hyperbolic model, the modified hyperbolic model, and the Ramberg-Osgood model to determine values of $R_{eq}$ for damping ratio. The results based on modified hyperbolic model varying curvature coefficient, a, show that the range of $R_{eq}$ is wider at higher strain levels than for other models. Changing soil parameters $(\alpha,b,\gamma_r)$ in Ramberg-Osgood model also caused scattered in value of $R_{eq}$ both low and high strains but not as significant as occurred at higher strain using modified hyperbolic model.

The actual soil damping has a significant component of nonhysteretic damping. In order to check the validity of the Sasanakul's $R_{eq}$ values for damping, the combined non-viscous hyperbolic model was employed. The results show identical values of $R_{eq}$ to those obtained by Sasanakul.

Finally, methods for application of the modified equivalent radius approach to RC/TS testing are presented. Two methods are presented for RC testing based upon the half power band width method and the free vibration decay method. And an approach for TS testing is presented.

## ACKNOWLEDEGEMENT

This project was supported by the Geotechnical Engineering Center at the Utah State University. Its support is greatly appreciated. Encouragement and help from Dr. Bay is gratefully acknowledged.

## REFERENCES

1. Chen, A.T. F., and Stokoe, K. H., II., *Interpretation of strain dependent modulus and damping from torsional soil tests*, Report No. USGS-GD-79-002, NTIS No. PB-298479, U.S. Geological Survey, 46, 1979, 45pp.
2. Sasanakul, I., "Development f an electromagnetic and mechanical model for a resonant column and torsional shear testing device for soils," PhD dissertation, Utah State University, Logan, Utah, 2005, 275pp.
3. Darendeli, M.B. and Stokoe, K.H., II., *Dynamic properties of soils subjected to the 1994 Northridge earthquake* Geotechnical Engineering Report GR97-5, Civil Engineering Department, University of Texas at Austin, 1997.
4. Ishihara, K., *Soil Behavior in Earthquake Geotechnics*, Oxford University Press, Oxford, 1996, 350pp.
5. Masing, G., "Eigenspannungen und Verfestgung Beim Masing," *Proceedings of the 2nd International Congress of Applied Mechnics*, 1926, pp. 332-335.
6. Kokushu, T., "In situ dynamic soil properties and their evaluation," *Proceedings of the 8th Asian Regional Conference on Soil Mechanics and Foundation Engineering*, 1987, pp. 215-435.
7. Seed, H. B., and Idriss, I. M., *Soil modulus and damping factors for dynamic response analyses*, Report No. EERC-70-10, Earthquake Engineering Research Center, Univ. of California, Berkeley, Calif., 37, 1970, 41pp.
8. Hardin, B. O., and Drnevich, V. P., "Shear modulus and damping in soils: measurement and parameter effects," *Journal of Soil Mechanics and Foundation*, ASCE, 98 (6), 1972, pp. 603-624.
9. Pyke, R.M., "Evolution of soil models since the 1970s," International Workshop on the Uncertainties in Nonlinear Soil Properties and their Impact on Modeling Dynamic Soil Response, University of California, Berkeley, 2004.
10. Sasanakul, I. and Bay, J.A., "Stress integration approach accounting for nonuniform stress-strain in resonant column and torsional shear testing for soils," *Journal of Geotechnical & Geoenvironmental Engineering*, 2008, in review
11. Bae, Y.S., "Modeling soil behavior in large strain resonant column and torsional shear tests, Utah State University, Logan, Utah, 2007, 184pp.
12. Idriss, I. M., Dobry, R., and Singh, R. D., "Nonlinear behavior of soft clays during cyclic loading," *Journal of Geotechnical Engineering*, ASCE, 104 (12), 1978, pp. 1427-1447.
13. Lin, M. L., Ni, S. H., Wright, S. G., and Stokoe, K. H., II., "Characterization of material damping in soil," *Proceedings of the 9th World Conference on Earthquake*, Tokyo-Kyoto, Japan, Vol 3, 1988, pp. 5-10.
14. Richart, F.E., Hall, J.R., and Woods, R.D., *Vibration of Soils and Foundations*, Prentice Hall, 1970, 414pp.